Determination of Aerodynamic Sensitivity Coefficients Based on the Transonic Small Perturbation Formulation

Hesham M. Elbanna* and Leland A. Carlson†
Texas A&M University, College Station, Texas 77843

The quasianalytical approach is developed to compute airfoil aerodynamic sensitivity coefficients in the transonic and supersonic flight regimes. Initial investigation verifies the feasibility of this approach as applied to the transonic small perturbation residual expression. Results are compared to those obtained by the direct (finite difference) approach, and both methods are evaluated to determine their computational accuracies and efficiencies. The quasianalytical approach is shown to yield more accurate coefficients and is potentially more efficient and worth further investigation.

Nomenclature

C = maximum camber in fraction of chord
Cp = pressure coefficient
IM, JM = grid dimensions
JB = row above airfoil
L = chordwise location of maximum camber
M = Mach number
R = residual expression
T = maximum thickness in fraction of chord
XD = design variable
f, g = Cartesian coordinate stretching functions
x, y = Cartesian coordinates
ξ, η = computational variables
α = angle of attack
γ = ratio of specific heats
Γ = circulation
φ = perturbation potential function
ΔCp = $Cp_l - Cp_u$

Subscripts

∞ = freestream condition
b = body
p = pressure
u, l = upper, lower
TE = trailing edge

Introduction

OVER the past few years, computational fluid dynamics has evolved rapidly as a result of the immense advancements in the computational field and the impact of the use of computers on obtaining numerical solutions to complex problems. Accordingly, researchers are now capable of calculating aerodynamic forces on wing-body-nacelle-empennage configurations. A next logical step would be to compute the sensitivity of these forces to configuration geometry.

In order to improve the design of transonic vehicles, design codes are being developed that use optimization techniques; and, in order to be successful, these codes require aerodynamic sensitivity coefficients, which are defined as the derivatives of the aerodynamic functions with respect to the design variables. Obviously, it is desirable that such sensitivity coefficients be easily obtained. Consequently, the primary objective of this effort is to investigate the feasibility of using the quasi-analytical method[1-3] for calculating the aerodynamic sensitivity derivatives in the transonic and supersonic flight regimes. As part of this work, the resulting sensitivity coefficients are compared to those obtained from the finite difference approach. Finally, both methods are evaluated to determine their computational accuracies and efficiencies.

In the transonic regime, a variety of flowfield solution methods exist. These range from full Navier-Stokes solvers to transonic small perturbation equation solvers. The complexity of the equations that need to be solved depends upon the flow phenomena in question and the objective of the analysis. Since it is not the objective of this work to develop flowfield algorithms, the present research uses the nonlinear transonic small perturbation equation to determine and verify efficient methods for calculating the aerodynamic sensitivity derivatives. In addition, only two-dimensional results will be presented in this initial work.

Background

Most recently, sensitivity methodology has been successfully used in structural design[2] and optimization programs[3] primarily to assess the effects of the variation of various fundamental properties relative to the important physical design variables. Moreover, researchers have developed and applied sensitivity analysis for analytical model improvement and assessment of design trends. In most cases, a predominant contributor to the cost and time in the optimization procedures is the calculation of derivatives. For this reason, it is desirable in aerodynamic optimization to have efficient methods of determining the aerodynamic sensitivity coefficients and, wherever possible, to develop appropriate numerical methods for such computations.

Currently, most methods for calculating transonic aerodynamic sensitivity coefficients are based upon the finite difference approximation to the derivatives. In this approach, a design variable is perturbed from its previous value, a new complete solution is obtained, and the differences between the new and the old solutions are used to obtain the sensitivity coefficients. This direct, or brute force, technique has the disadvantage of being potentially very computer intensive, especially if the governing equations are expensive to solve. In addition, it is difficult to guarantee the accuracy of the derivatives obtained by the finite difference method. Accordingly, the need to eliminate these costly and repetitive analyses is the primary motivation for the development of alternative, efficient computational methods to determine the aerodynamic sensitivity coefficients.

Presented as Paper 89-0532 at the AIAA 27th Aerospace Sciences Meeting, Reno, NV, Jan. 9-12; received March 15, 1989; revision received Oct. 2, 1989.

*Graduate Research Assistant. Student Member AIAA.
†Professor, Aerospace Engineering. Associate Fellow AIAA.

Problem Statement

Based on the foregoing discussion, the current problem is formulated starting from the generic quasianalytical approach and manipulated according to the rules given in Appendix A of Ref. 1 for the derivation of the general sensitivity equation. This general sensitivity equation is then applied to the residual expression R of the transonic small perturbation equation, which is a simple and adequate description of the nonlinear phenomena occurring in the transonic regime. Although this expression is nonlinear in the perturbation potential φ, the general sensitivity equation, Eq. (1), is linear with respect to the unknown sensitivity ($\partial\varphi/\partial XD_i$). It is to be noticed that the practical implementation of the above step is not achieved until the residual expression is approximated on a finite domain and the mathematical form of the problem rendered to that of one in linear algebra. This discretization process is explained in detail in Ref. 4.

Thus, the quasianalytical method, as applied to the residual expression of the transonic small perturbation equation, yields the sensitivity equations,

$$\left[\frac{\partial R}{\partial \varphi}\right]\left\{\frac{\partial \varphi}{\partial XD_i}\right\} = -\left\{\frac{\partial R}{\partial XD_i}\right\} \tag{1}$$

where

$$R \equiv (B_1 + B_2\varphi_x)\varphi_{xx} + \varphi_{yy} = 0 \tag{2}$$

$$B_1 = 1 - M_\infty^2$$

$$B_2 = -(\gamma+1)M_\infty^2$$

$$\varphi \equiv \varphi(x,y,XD) \tag{3}$$

$XD \equiv$ set of design variables

$XD_i \equiv i$th design variable

subject to the airfoil boundary condition,

$$\varphi_y(x_b,0) = \left[\frac{dy}{dx}\right]_b = F(x,XD) \tag{4}$$

the infinity boundary condition, for $M_\infty < 1$

$$\varphi_\infty = -\Gamma\theta/(2\pi), \qquad \theta = n\pi/2, \qquad n = 0,1,2,3,4$$

or for $M_\infty > 1$

$$\varphi_\infty = 0, \qquad \theta = n\pi/2, \qquad n = 1,2,3$$

$$\varphi_x = 0, \qquad \theta = n\pi/2, \qquad n = 0,4 \tag{5}$$

and the Kutta condition

$$\Delta P = 0 \qquad (\Gamma = \Delta\varphi = \text{const}), \qquad x_{TE} < x \le \infty \tag{6}$$

Equation (1) is discretized into a system of linear equations to be solved for the unknown sensitivity vectors. In carrying out this step, the expressions for both the right side vector and the left side matrix are generated analytically. The solution of this system is obtained efficiently by using either a direct or an iterative procedure that allows for multiple right sides. This approach is explained in the following section and has the advantage that several unknown vectors can be obtained simultaneously, each vector representing the sensitivity of the potential φ with respect to some design variable XD_i.

At this stage, it is convenient to define the vector of design variables

$$XD = \{XD_1, XD_2, \ldots, XD_n\} \tag{7}$$

and to exactly determine which variables influence the solution of Eq. (2). In doing so, the relation between the sensitivity coefficients corresponding to these variables and the form of the optimization algorithm that utilizes this information needs to be considered. Notice that the derivatives computed in this study, namely, the first partial derivatives, are adequate for a typical optimization routine if it were to be applied to the present two-dimensional problem. Notice also that some optimization studies might require higher derivatives.

For the transonic flow problem, an appropriate choice of the first design variable is the freestream Mach number (M_∞). This variable appears in the governing Eq. (2) and has an important influence on the character of the equation via its influence on local Mach number (for $M<1$, the equation is elliptic, for $M>1$, the equation is hyperbolic) and thus on the nature of the solution. For this reason, it is desirable to have M_∞ as one of the design variables.

Next, it is appropriate to examine the boundary condition given by Eq. (4). In the transonic small perturbation formulation, the angle of attack (α) enters the problem through the boundary condition and thus,

$$F_{u_1} = \left[\frac{dy}{dx}\right]_b = y'_{u_1} - \alpha \tag{8}$$

For simplicity, the function F should be easily differentiable with respect to the design variables defining the airfoil geometry. This desirable feature simplifies the computation of the right side term of the sensitivity equation. Therefore, it would seem plausible to have a simple analytical expression for modeling the upper and lower surfaces of the airfoil.

For the present studies, it was decided to limit consideration to one basic airfoil section, namely the NACA four-digit section, whose families of wing sections are obtained by combining a mean line and a thickness distribution.[5] The resultant expressions possess the necessary features that suit the problem, mainly the concise description of the airfoil surfaces in terms of several geometric design variables. The expressions are as follows:

$$y_{u_1} = \begin{cases} C(2Lx - x^2)/L^2 \pm 5T(0.2969\sqrt{x} - 0.126x \\ \quad -0.3516x^2 + 0.2843x^3 - 0.1015x^4), \quad x \le L \\ C[(1-2L) + 2Lx - x^2]/(1-L)^2 \\ \quad \pm 5T(0.2969\sqrt{x} - 0.126x - 0.3516x^2 \\ \quad +0.2843x^3 - 0.1015x^4), \quad x > L \end{cases} \tag{9}$$

Each of the quantities C, L, and T is expressed as a fraction of the chord. Differentiating Eq. (9) with respect to x and substituting the result into Eq. (8) yields

$$F_{u,1} = 2C(L-x)/LL \pm 5T(0.14845/\sqrt{x} - 0.126 - 0.7032x + 0.8529x^2 - 0.406x^3) - \alpha \tag{10}$$

where

$$LL = \begin{cases} L^2, & x \le L \\ (1-L)^2, & x > L \end{cases} \tag{11}$$

Eq. (10) is a simple analytical expression in terms of the four variables T, L, C, and α. Thus,

$$XD = \{T,\ M_\infty,\ \alpha,\ L,\ C\} \tag{12}$$

represents the complete set of design variables that define the present two-dimensional airfoil sensitivity problem. Notice that these variables are completely uncoupled; and, thus, the sensitivity equation can be solved independently with respect to each variable.[6]

Mathematical Treatment and Solution Procedure

Problem Discretization

Equation (1) represents the general sensitivity equation applied to the residual R. Now, in order to solve the problem numerically, Eq. (2) is formulated computationally on a finite domain. This transformation is achieved by using a stretched Cartesian grid that maps the infinite physical domain onto a finite computational grid. In this study, the grid used is based upon a hyperbolic tangent transformation that places the outer boundaries at infinity. Accordingly, the transformed residual expression is given by

$$R \equiv [B_1 + B_2 f\varphi_\xi] f(f\varphi_\xi)_\xi + g(g\varphi_\eta)_\eta = 0 \tag{13}$$

This equation is solved numerically by an approximate factorization scheme.[7] In finite-difference form, Eq. (13) can be written as

$$\begin{aligned} R_{i,j} \equiv & \left[B_1 + B_2(\varphi_{i+1,j} - \varphi_{i-1,j}/(2\Delta\xi)\right] f_i/\Delta\xi^2 \\ & \times \left[\nu_{i,j} f_{i+\frac{1}{2}}(\varphi_{i+1,j} - \varphi_{i,j}) - (2\nu_{i,j} - 1) f_{i-\frac{1}{2}}(\varphi_{i,j} - \varphi_{i-1,j})\right. \\ & \left. - (1 - \nu_{i,j}) f_{i-3/2}(\varphi_{i-1,j} - \varphi_{i-2,j})\right] \\ & + \left[g_{j+\frac{1}{2}}(\varphi_{i,j+1} - \varphi_{i,j}) - g_{j-\frac{1}{2}}(\varphi_{i,j} - \varphi_{i,j-1})\right] g_j/\Delta\eta^2 \end{aligned} \tag{14}$$

where

$$\nu_{i,j} = 1 \quad \text{if point } (i,j) \text{ is subsonic}$$

$$\nu_{i,j} = 0 \quad \text{if point } (i,j) \text{ is supersonic}$$

Eq. (14) is the discretized form of the residual at a general point (i,j) in terms of φ values at surrounding points. Consequently, R at i,j can be viewed as a function of the φ values at neighboring points; and, therefore, the differentiation of the residual expression is straightforward.

Differentiation of the Residual

Rearranging Eq. (14) yields

$$\begin{aligned} R_{i,j} = & c_1\varphi_{i,j} + c_2\varphi_{i+1,j}\varphi_{i-1,j} + c_3\varphi_{i+1,j}\varphi_{i,j} + c_4\varphi_{i-1,j}\varphi_{i,j} \\ & + c_5\varphi_{i+1,j}\varphi_{i-2,j} + c_6\varphi_{i-1,j}\varphi_{i-2,j} + c_7\varphi_{i-1,j}^2 + c_8\varphi_{i+1,j}^2 \\ & + c_9\varphi_{i+1,j} + c_{10}\varphi_{i-1,j} + c_{11}\varphi_{i,j+1} + c_{12}\varphi_{i,j-1} + c_{13}\varphi_{i-2,j} \end{aligned} \tag{15}$$

The coefficients $c_1, c_2, \ldots, c_{13}$ are functions only of the stretching factors and of B_1 and B_2, which are functions of M_∞. This fact is used when differentiating Eq. (15) with respect to M_∞ in order to obtain the right side $(\partial R/\partial M_\infty)$. It is also necessary to consider the treatment of various types of grid points and examine the effect on the general residual expression. Several groups of points, such as those adjacent to the airfoil, to the wake cut, and to infinity boundaries, need special treatment. Accordingly, it is necessary to revise the residual expression at these boundary points to include the boundary conditions. The resulting updates are then used to modify the residual equation, Eq. (15), and to yield a set of expressions, each being valid for a group of boundary points. The details of these operations and the expressions for the coefficients c_1–c_{13} are found in Ref. 4.

In setting up the complete quasianalytical problem, the circulation and its dependence upon trailing-edge potentials must be carefully included. Since the circulation is determined by the difference in potentials at the trailing edge,

$$\Gamma = \varphi_{u\text{TE}} - \varphi_{\text{ITE}} \tag{16}$$

or, by interpolating the trailing-edge values

$$\begin{aligned} \Gamma = & T_1\left[1.5(\varphi_{\text{ITE}-1,JB} - \varphi_{\text{ITE}-1,JB-1})\right. \\ & \left. - 0.5(\varphi_{\text{ITE}-1,JB+1} - \varphi_{\text{ITE}-1,JB-2})\right] \\ & + T_2\left[1.5(\varphi_{\text{ITE},JB} - \varphi_{\text{ITE},JB-1})\right. \\ & \left. - 0.5(\varphi_{\text{ITE},JB+1} - \varphi_{\text{ITE},JB-2})\right] \end{aligned} \tag{17}$$

where

$$T_2 = \left[\xi(x = 0.5) - \xi(\text{ITE} - 1)\right]/\Delta\xi \tag{18}$$

$$T_1 = [1 - T_2] \tag{19}$$

and since a branch cut extends from the trailing edge to downstream infinity, and trailing-edge potentials appear in the residual expressions for points along the branch cut. In addition, since in the two-dimensional case the infinity boundary conditions are proportional to the circulation, the trailing-edge potentials also appear in the residual expressions at points adjacent to the outer boundaries. Consequently, the resultant matrix $(\partial R/\partial\varphi)$, while banded, also contains many nonzero elements far from the central band. Notice that the presence of these elements greatly complicates the rapid and efficient solution of the sensitivity equation, Eq. (1).

The resulting residual expressions are differentiated analytically with respect to the potential φ. Specifically, each equation is differentiated with respect to the potential at neighboring points and trailing-edge points. The latter enter as a result of the implicit nature of the circulation effects. These points are denoted by the counters (ii,jj) and are given by

$$(i,j-1),\ (i,j),\ (i,j+1),\ (i-2,j),\ (i-1,j),\ (i+1,j)$$

$$(\text{ITE}-1,JB-2),\ (\text{ITE}-1,JB-1),\ (\text{ITE}-1,JB)$$

$$(\text{ITE}-1,JB+1),\ (\text{ITE},JB-2),\ (\text{ITE},JB-1)$$

$$(\text{ITE},JB),\ (\text{ITE},JB+1)$$

Solution about a Fixed Design Point

Once the residual relations are obtained, the actual coefficients are assembled by evaluating the appropriate analytical expressions using a flowfield solution obtained from Eq. (2) for a given set of conditions (i.e., about a fixed design point). Similarly, the right sides are evaluated by differentiating the analytical expressions for the residual with respect to each design variable. Again, the details and results of these steps are found in Ref. 4.

The end result is that the coefficient matrix $(\partial R_{i,j}/\partial\varphi_{ii,jj})$ is of size $(IM-2)\times(JM-2)\times(IM-2)\times(JM-2)$ for a general $(IM \times JM)$ grid. This system is large, of block structure, diagonally dominant, and sparse and, while banded, also contains many nonzero elements far from the central band. As a result of this size and structure, it is obvious that a reasonably fast scheme for solving Eq. (1) is needed.

Currently, it is very difficult to single out an optimum routine that handles a general, large, sparse system of linear equations for which the coefficient matrix is unsymmetric. This is because, unlike the theory of symmetric matrices, the theory of general unsymmetric matrices is more involved and has yet to be developed. Since research in the above areas is currently very active and specialized, any attempt to cover these topics in detail would be laborious. For this reason, it was decided to use a few general but not necessarily the most efficient approaches that were available in the literature and that could be integrated into the sensitivity codes with adjustments. This approach would allow an evaluation of the overall cost involved in solving the current two-dimensional problem.

The first solver is based on standard Gaussian elimination with partial pivoting and full storage. The second is based on triangular decomposition[8] and uses a compact storage scheme that avoids handling the zero entries and therefore should be more efficient than standard Gaussian elimination. The third solver is based on a Gauss-Seidel iterative scheme[9] and was not optimized for speed (through the choice of optimum acceleration parameters) but uses sparse matrix technology in processing only the nonzero elements. The fourth and last solver used is based on the conjugate gradient method.[10] Handling the sparsity pattern for the third and fourth solvers is achieved by assembling the symbolic part of the coefficient matrix only once for a given grid size and given freestream (subsonic vs supersonic). The resultant structure is then stored on a disk file. Before the numerical part is executed, the symbolic information is read into the code and used directly to assemble the new matrix. This procedure is followed to reduce the time consumed in assembling the coefficient matrix. Notice also that in the Gauss-Seidel and conjugate-gradient solvers that the error tolerances for the coefficients involving maximum thickness, freestream Mach number, and location of maximum camber were 1.E-06, while those on angle of attack and maximum camber were 1.E-04.

Once the sensitivities of the potentials, and thus the Cp distribution, to the design variables are known, the sensitivity of the lift coefficients to the design variables can be easily computed. To minimize errors, these coefficients are computed using

$$C_L = 2\Gamma = 2(\varphi_{u\mathrm{TE}} - \varphi_{\mathrm{ITE}}) \tag{20}$$

and hence,

$$\partial C_L/\partial XD_i = 2(\partial\varphi_{u\mathrm{TE}}/\partial XD_i - \partial\varphi_{\mathrm{ITE}}/\partial XD_i) \tag{21}$$

Finally, all methods used for computing the derivatives are compared to the finite-difference approach, and the results are presented and evaluated to determine the computational accuracy and efficiency of each method.

Test Cases

In this study, the quasianalytical method has been used to determine the aerodynamic sensitivity coefficients at two freestream Mach numbers ($M_\infty = 0.2, 0.8$) for the NACA 1406 airfoil at 1-deg angle of attack. Results were also obtained[4,11] for a supersonic case at $M_\infty = 1.2$. Notice that further studies are needed to examine the results for a wider range of design parameter variation.

In the following, two types of results will be presented. The first will be plots of Cp vs chord for the three chosen Mach numbers. The second will be the corresponding plots of $(\partial Cp/\partial T)$, $(\partial Cp/\partial M_\infty)$, $(\partial Cp/\partial\alpha)$, $(\partial Cp/\partial C)$, and $(\partial Cp/\partial L)$ for the upper and lower surfaces and plots of $(\partial\Delta Cp/\partial T), \ldots$, etc., involving the difference, all will be obtained by the quasianalytical method. In addition, all of the figures will also contain results obtained using the direct (finite difference) approach in which each design variable was individually perturbed by a small amount, typically 0.001, and a new flowfield solution obtained. Then the sensitivities were computed using $\Delta Cp/\Delta XD$ and are shown via dashed lines. In many cases, the lines are coincident with the quasianalytical results and cannot be observed. Table 1 compares results obtained by the two methods, and in most cases the agreement is within 1%.

In all cases, an 81×20 stretched Cartesian grid was utilized. While finer grid studies are needed, they were not performed as part of this initial study. In addition, for these studies, the flowfield was normally computed using double precision arithmetic and the maximum residual reduced eight orders of magnitude. It was felt that this level of convergence was necessary in order to accurately evaluate sensitivity coefficients using a finite-difference approach, although such convergence may not be required in the flowfield solver for the quasi-analytical method.

Table 1 Accuracy of quasianalytical method for computing lift coefficient sensitivity derivatives for NACA 1406, GRID 81×20

XD_i	Method[a]	$M_\infty = 0.2$	$M_\infty = 0.8$	$M_\infty = 1.2$
T	FD	0.0044	0.5232	−0.2949
	QA	0.0044	0.5447	−0.3376
M_∞	FD	0.0471	0.9708	1.0235
	QA	0.0470	0.9905	−0.0703
α	FD	6.1385	10.5229	4.8758
	QA	6.1386	10.5229	4.8726
C	FD	9.9380	19.5767	0.7695
	QA	9.9381	18.6154	0.7356
L	FD	0.0696	0.1499	−0.0348
	QA	0.0693	0.1496	−0.0349

[a]FD, finite difference. QA, quasianalytical.

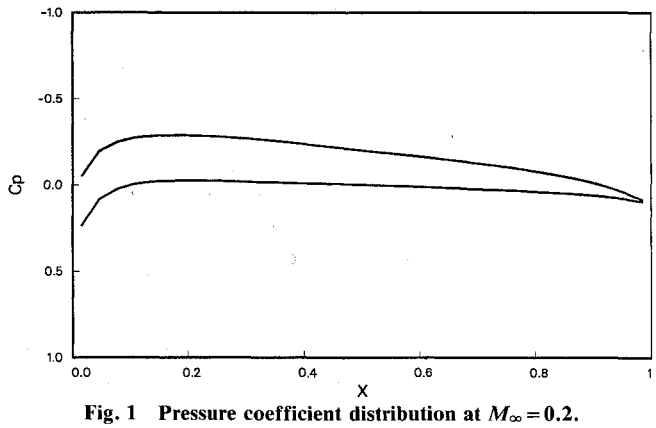

Fig. 1 Pressure coefficient distribution at $M_\infty = 0.2$.

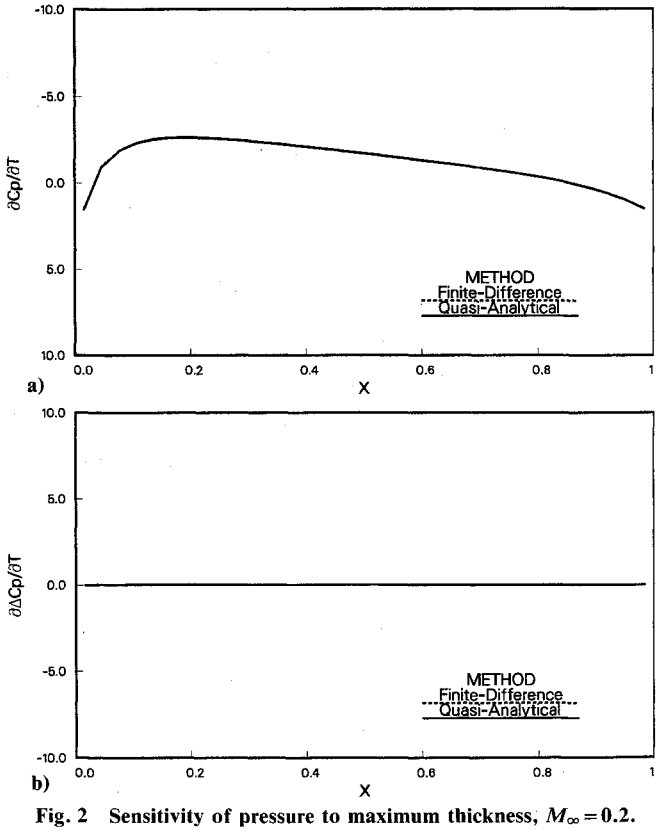

Fig. 2 Sensitivity of pressure to maximum thickness, $M_\infty = 0.2$.

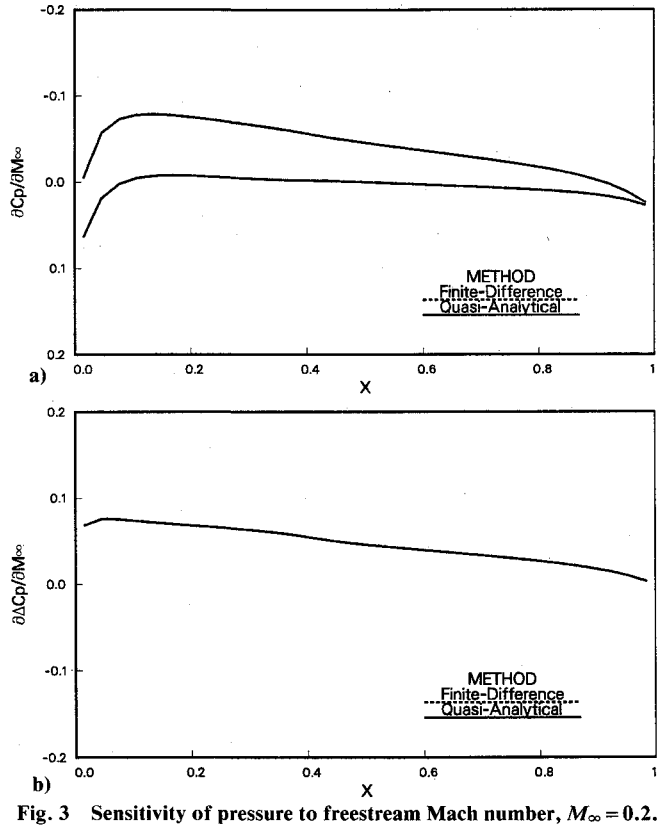

Fig. 3 Sensitivity of pressure to freestream Mach number, $M_\infty = 0.2$.

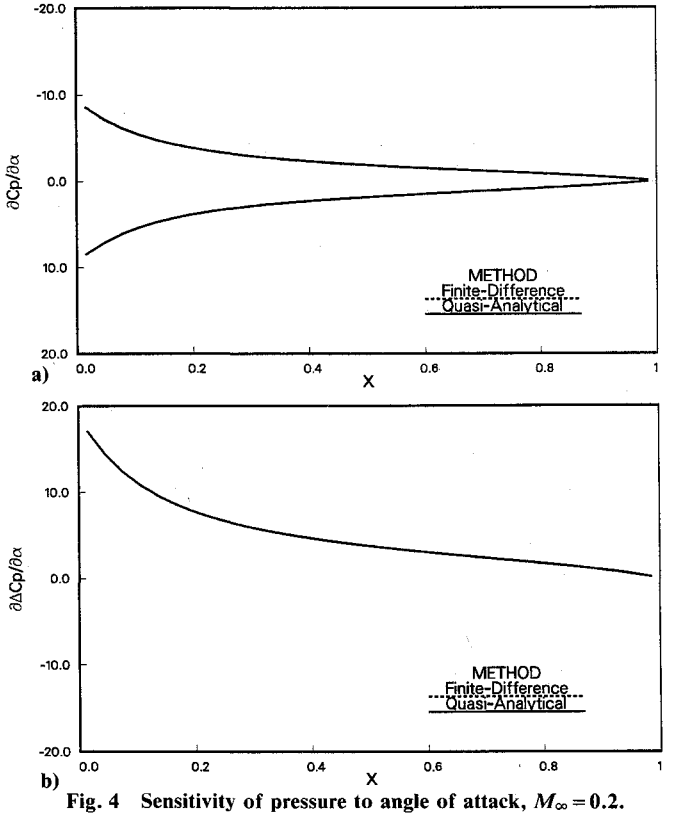

Fig. 4 Sensitivity of pressure to angle of attack, $M_\infty = 0.2$.

Results and Discussion

Subsonic Case – $M_\infty = 0.2$

Initial studies concentrated on subsonic cases since at least approximate results would be known from thin airfoil theory.[5] Figure 1 shows the pressure distribution for the NACA 1406 airfoil, while Figs. 2a and 2b show the sensitivity of the pressure to thickness for the same airfoil. As expected from thin

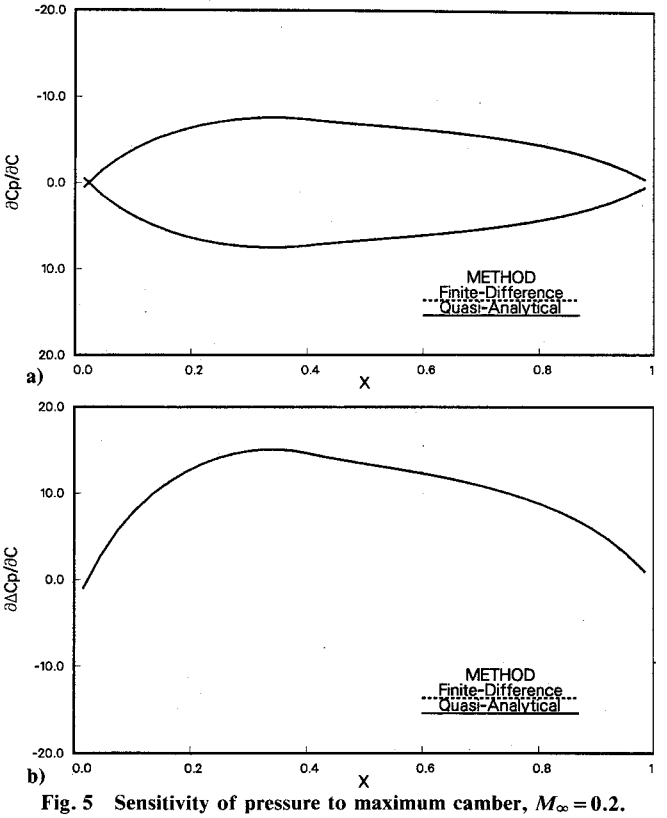

Fig. 5 Sensitivity of pressure to maximum camber, $M_\infty = 0.2$.

airfoil theory, the upper and lower surface values are essentially identical, and the difference is very small everywhere. Also shown on the same figure (and on subsequent figures) by the dashed line is the result obtained by using the finite-difference approach; and as can be seen, the agreement between the two approaches is excellent.

The sensitivity of pressure to freestream Mach number is plotted on Figs. 3a and 3b. It is noticed that while the profiles for the upper and lower surfaces are similar, they are not equal in magnitude, indicating a nonlinear variation with Mach number as predicted by simple Prandtl-Glauert theory. However, as indicated by the results plotted on Fig. 3b, the magnitudes for this subsonic Mach number are very low.

The sensitivity of the pressure coefficients to angle of attack are depicted for this case in Figs. 4a and 4b. As expected from linear thin airfoil theory, the upper and lower surface curves are essentially equal in magnitude but of opposite sign. Not surprisingly, the sensitivity of the delta Cp variation, Fig. 4b, has the shape of the pressure difference curve for a flat plate at angle of attack; and its magnitude, particularly near the leading edge, is quite large.

On Figs. 5a and 5b is plotted the sensitivity of the pressure coefficient to the amount of maximum camber. Since camber contributes to lift, it is expected from the thin airfoil theory that these values should be "equal but opposite in sign" for the upper and lower surfaces. In addition, the pressure difference curve has the correct shape for that associated with a 14 mean line with the peak occurring at 30% chord[5] and has a magnitude comparable to those for the $(\partial Cp/\partial\alpha)$ curves.

Finally, the sensitivity of pressure to the location of the maximum camber point is portrayed in Figs. 6a and 6b and, to say the least, the results are interesting. Since maximum camber location affects the camber profile and hence lift, the equal and opposite behavior of the upper and lower surface coefficients is expected. In addition, the pressure difference sensitivity is primarily negative forward of the point of maximum camber and positive aft of it. This result indicates that if the location of maximum camber were moved rearward slightly (i.e., a positive ΔL), that lift would be decreased on the forward portion of the airfoil and increased on the aft portion of

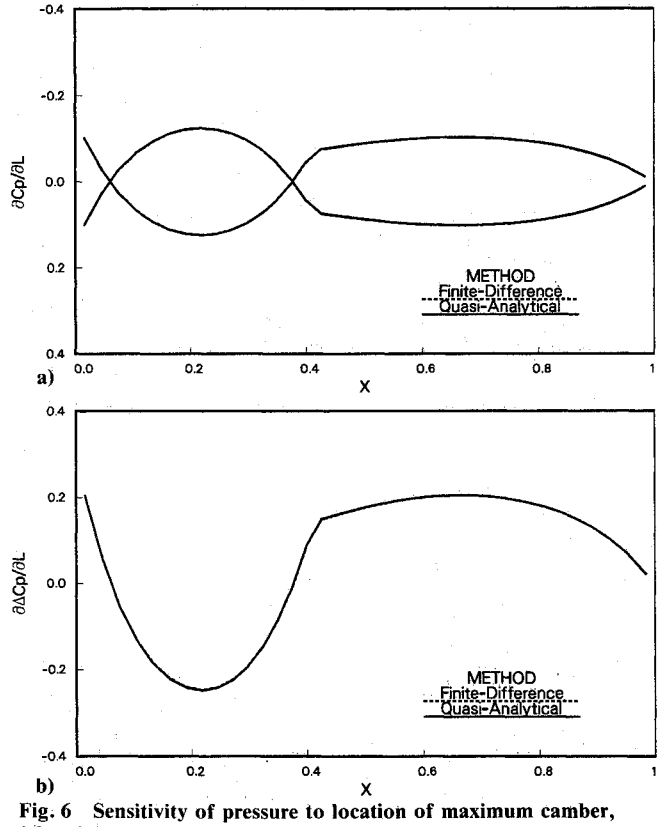

Fig. 6 Sensitivity of pressure to location of maximum camber, $M_\infty = 0.2$.

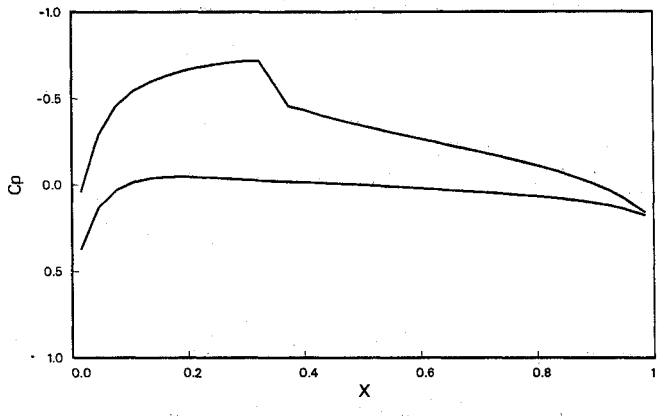

Fig. 7 Pressure coefficient distribution at $M_\infty = 0.8$.

the airfoil, which is in agreement with the results presented in Ref. 5.

Transonic Case – $M_\infty = 0.8$

At $M_\infty = 0.8$, the flow about the NACA 1406 airfoil has a strong shock at 40% chord, see Fig. 7, and the lower surface is entirely subcritical. As a consequence, the variation with chord of the sensitivity coefficients is considerably different than in the subsonic case.

Figs. 8a and 8b show the sensitivity of pressure to the maximum thickness; and while the lower surface profile is similar to that obtained at subsonic conditions, the upper surface curve and the pressure difference coefficient plot show the effect of the upper surface shock wave. The large peak on the curves corresponds to the location of the shock wave and indicates that the shock-wave location is very sensitive to maximum thickness. Notice on Figs. 8a and 8b the excellent agreement of the quasianalytical results indicated by the solid lines with those obtained using the finite-difference approach (dashed lines).

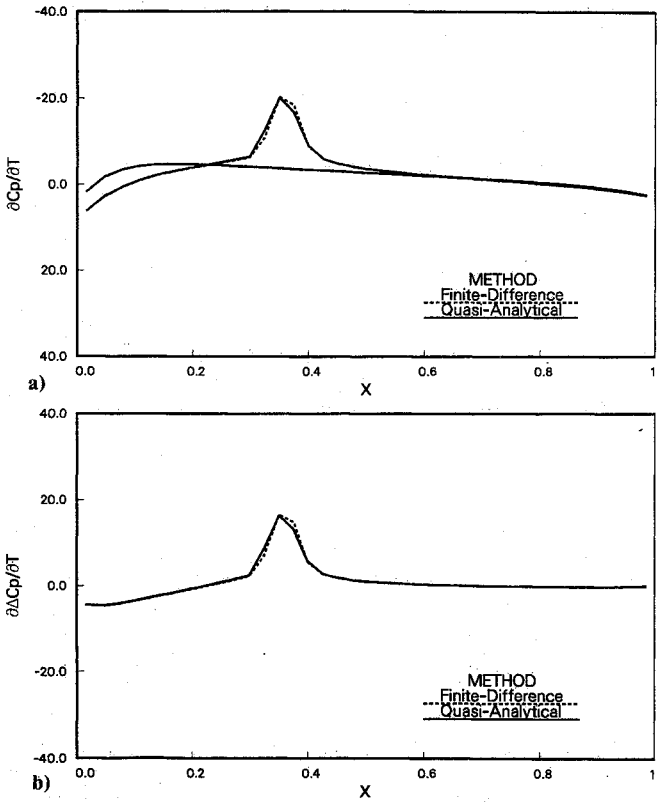

Fig. 8 Sensitivity of pressure to maximum thickness, $M_\infty = 0.8$.

The results for $(\partial Cp/\partial M_\infty)$, which are shown on Figs. 9a and 9b, are similar. The lower surface curve is typical of a subsonic flow, whereas the upper surface and the pressure difference coefficients reflect the presence of the upper surface shock wave. Similar comments can be made for the remaining design variable coefficients, which are plotted on Figs. 10, 11, and 12.

Examination of the curves in the vicinity of the shock wave location indicates that the pressure sensitivity and indirectly the shock wave location is about equally influenced by the maximum thickness, freestream Mach number, and angle of attack. However, in comparison it is relatively insensitive to the location of maximum camber; but, perhaps surprisingly so, the pressure is twice as sensitive to the amount of maximum camber as it is to the other design variables. It should also be noticed that the lift is most sensitive to angle of attack and to maximum camber.

In addition, Fig. 11 shows a discrepancy between the results obtained by the direct approach and those obtained through the quasianalytical method. It will be shown in the following section that this discrepancy is related to the choice of the step size used in computing the finite-difference solution, thus, revealing a significant deficiency in computing the sensitivity derivatives in nonlinear regimes via the finite-difference approach.

Time Comparisons

Obviously, in the development of the quasianalytical method, it was hoped that not only would this approach yield accurate values for the aerodynamic sensitivity coefficients, but also that it would be more efficient than the brute-force, finite-difference approach. Table 2 presents some comparisons concerning the amount of computational effort required to obtain solutions by the two approaches including results for the supersonic case.[4,11]

In comparing the values, several items should be kept in mind. First, it has been assumed that the finite-difference approach will require six independent solutions. In practice, it might be possible to start each finite-difference solution from

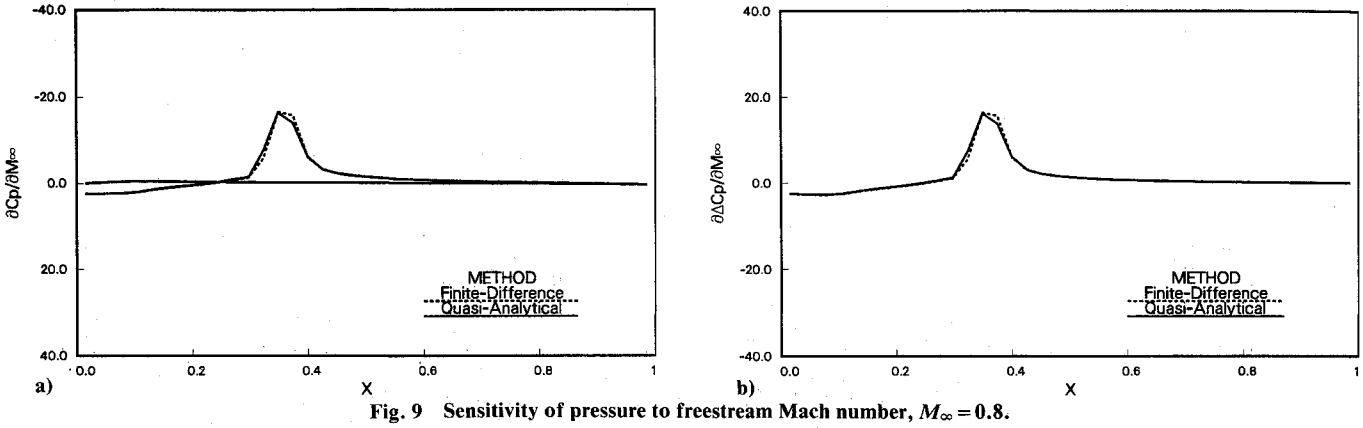

Fig. 9 Sensitivity of pressure to freestream Mach number, $M_\infty = 0.8$.

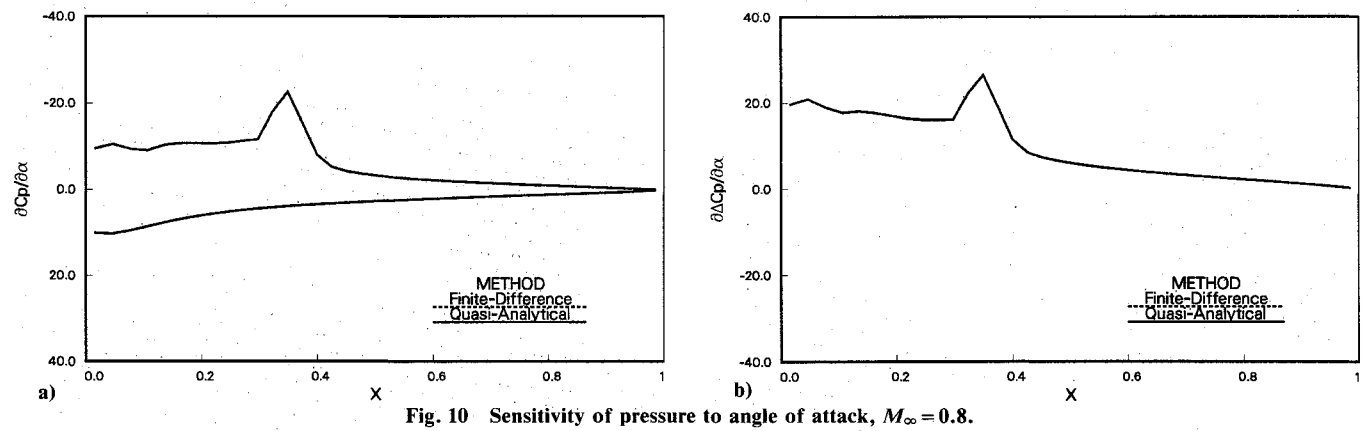

Fig. 10 Sensitivity of pressure to angle of attack, $M_\infty = 0.8$.

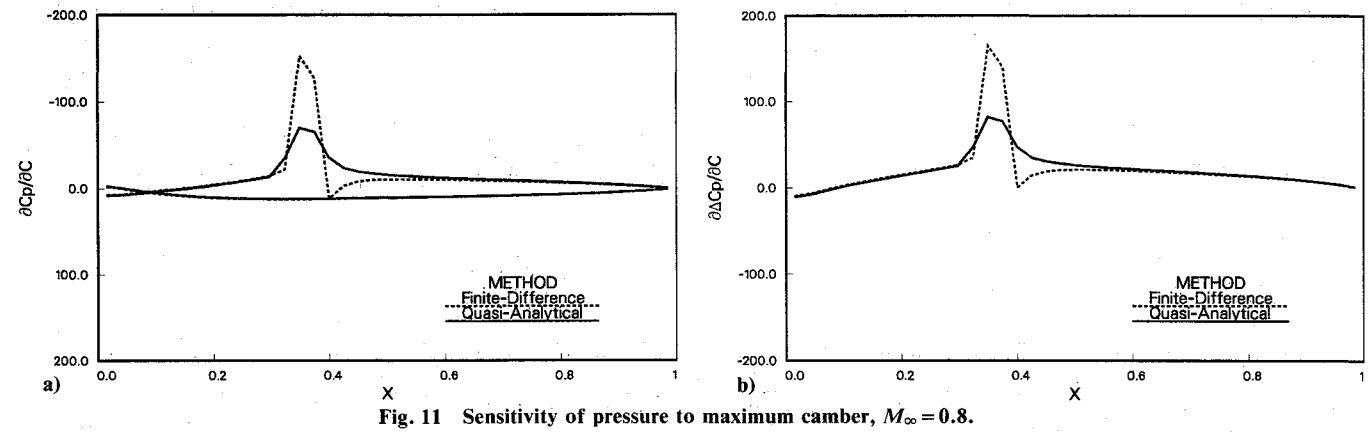

Fig. 11 Sensitivity of pressure to maximum camber, $M_\infty = 0.8$.

a previous solution and, thus, decrease the time to convergence. However, to be accurate, the finite-difference approach will probably require double precision and will have to be extremely well converged (i.e., 1.E-08). Nevertheless, the values for the finite-difference approach probably should be viewed as maximum values.

Second, the methods used for obtaining the sensitivity coefficients have not been optimized and, as mentioned earlier, may not even be optimum; and the flowfield solution required for the quasianalytical approach may not need double precision and may not have to be as tightly converged. Thus, the values shown for the quasianalytical approach should also be viewed as maximum values.

In spite of these limitations, results obtained by direct methods do indicate that the quasianalytical method is more computationally efficient at supersonic conditions and potentially efficient at transonic conditions than the brute-force, finite-difference approach.

Notice that in this study, the initial guess used in computing the sensitivity derivatives via iterative methods was arbitrarily chosen as the zero vector. In addition, time comparisons presented in Table 2 show that iterative methods are in general less efficient than direct methods if the derivatives for the current two-dimensional problem were sought about some general design point. However, if the objective is to incorporate the sensitivity derivatives into an optimization loop (i.e., to use the derivatives in a continuation problem), then, a good initial guess (which in that case would be available) would enhance convergence, and the overall cost of computing the derivatives using iterative methods might be reduced. These points should be taken into consideration when a sensitivity study is to be integrated into an optimization procedure.

Additional Test Cases

The first group of cases are carried out to investigate the performance of the NACA 1406 airfoil for a range of Mach numbers from 0.79 to 0.86 in increments of 0.01. As shown in Fig. 13, this range of transonic Mach numbers encompasses the development of the shock wave on the upper surface of the airfoil. Also, as shown on Figs. 14 and 15 for the cases involving thickness, Mach number, and maximum camber, the quasianalytical derivatives are in the vicinity of the shock wave frequently different from those obtained by the finite-difference approach. This discrepancy raises two questions—what is

Table 2 Time[a] comparisons for obtaining sensitivity coefficients for five design variables for NACA 1406, GRID 81×20

Method[b]	$M_\infty = 0.2$	$M_\infty = 0.8$	$M_\infty = 1.2$
FD	1.0000	1.0000	1.0000
TD	2.5187	0.9962	0.3929
GE	2.4089	0.9927	0.5165
GS	0.9971	1.5410	—
CG	35.2264	10.6199	—

[a]All CPU times were normalized by the time taken to compute FD derivatives.
[b]FD, finite difference; TD, triangular decomposition; GE, Gauss elimination; GS, Gauss-Seidel; CG, conjugate gradient.

Table 3 Effect of changing step size delta on finite-difference lift coefficient sensitivity derivatives for NACA 1406, GRID 81×20, $M_\infty = 0.84$

Delta XD_i	$XD_i = T$	$XD_i = M_\infty$	$XD_i = C$
1.E-03	7.7603	7.8715	24.0912
1.E-04	−0.8493	−0.6340	83.9853
1.E-05	−0.8497	−0.6364	14.7719
1.E-06	−0.8498	−0.6366	14.7695
QA[a]	−0.8498	−0.6367	14.7692

[a]QA, quasianalytical lift coefficient sensitivity derivatives.

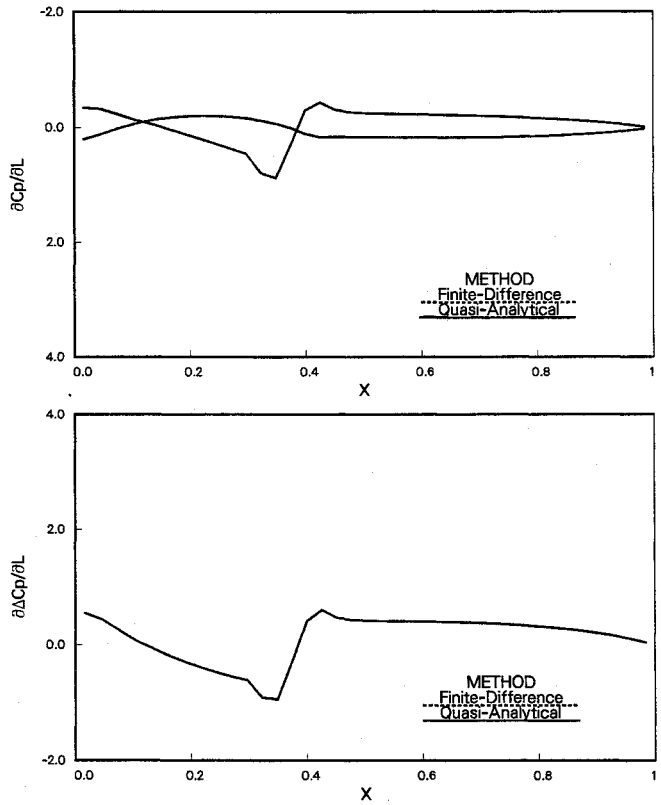

Fig. 12 Sensitivity of pressure to location of maximum camber, $M_\infty = 0.8$.

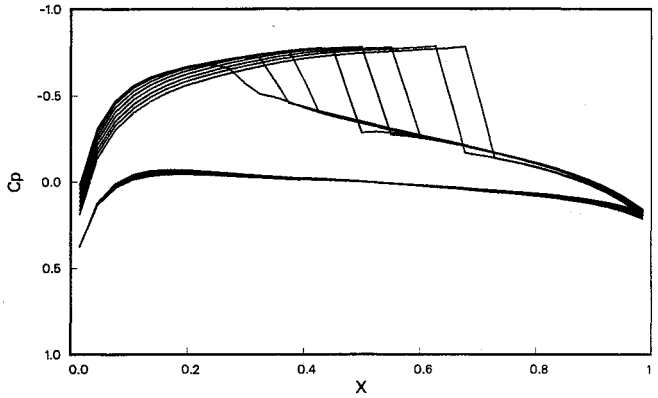

Fig. 13 Pressure coefficient distributions at various Mach numbers.

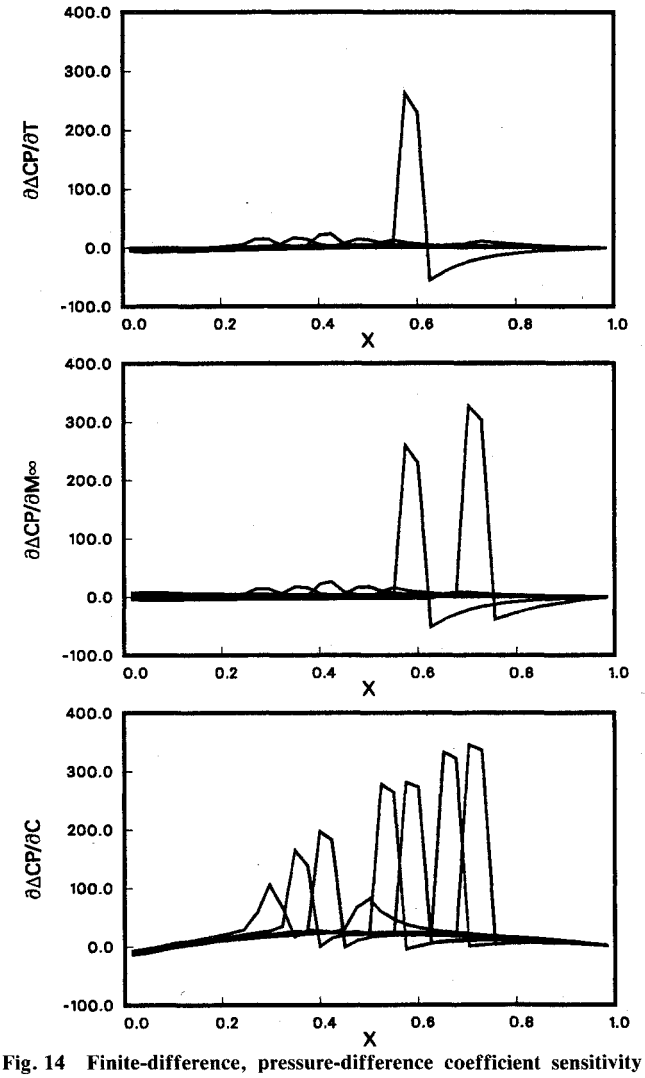

Fig. 14 Finite-difference, pressure-difference coefficient sensitivity derivatives at various Mach numbers.

the cause of the disagreement and which set of derivatives is more accurate? Examination of the variation of the integrated coefficient, $\partial CL/\partial XD_i$ with M_∞, which is portrayed on Fig. 16, shows that the quasianalytical results are smooth and follow a definite trend, whereas the finite-difference values are at best "discontinuous." Consequently, it is concluded that the finite-difference results are less accurate.

In order to observe the performance of the finite-difference approach in the transonic regime, it is necessary to examine the effect of changing the step size (delta of the design variable) on the computed derivatives. Four different values for the step size (1.E-03, 1.E-04, 1.E-05, and 1.E-06) were chosen and applied to the NACA 1406 at a Mach number of 0.84. Examination of this second group of results (see Table 3) show that as the step size is decreased, the finite-difference lift coefficient sensitivity derivatives approach the values computed by the quasianalytical method. However, in some cases, for small ΔXD_i values, oscillations in the pressure coefficient sensitivity derivatives have been observed depending upon the machine used and the method of storing and retrieving the data. These oscillations combined with the difficulty of properly choosing a suitable finite-difference ΔXD_i a priori indicates that the finite-difference approach is probably not a practical method of efficiently computing sensitivity coefficients. On the other

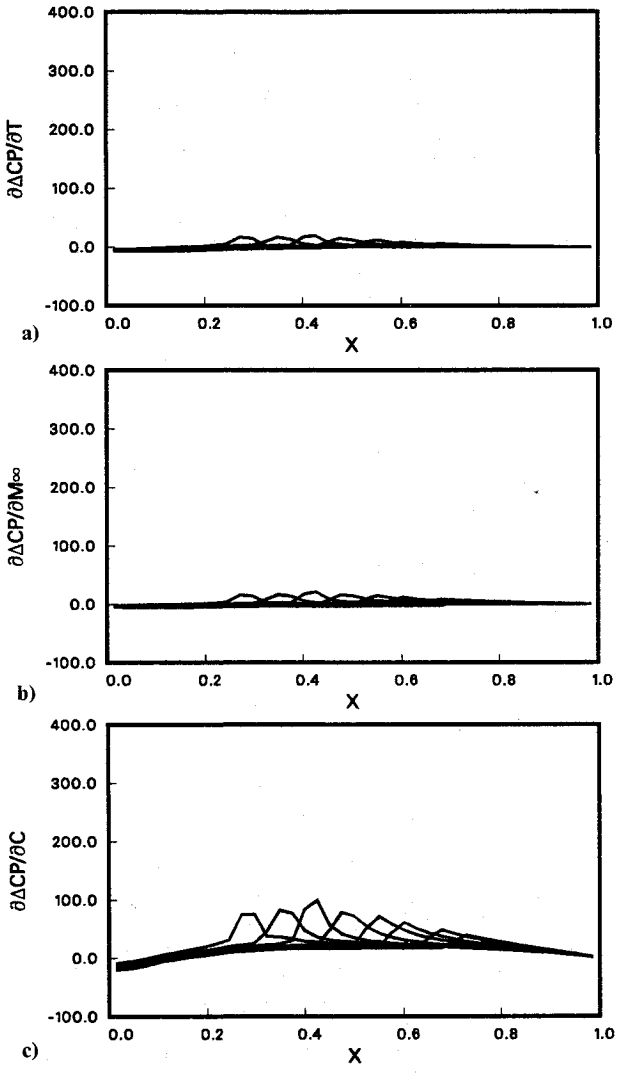

Fig. 15 Quasianalytical pressure-difference coefficient sensitivity derivatives at various Mach numbers.

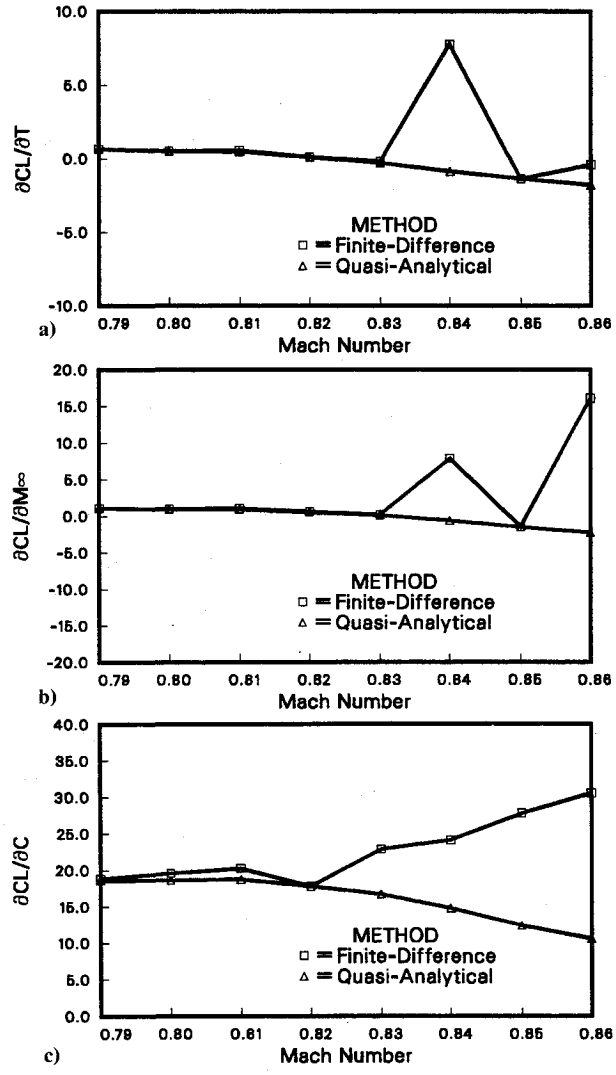

Fig. 16 Lift coefficient sensitivity derivatives.

hand, the present results demonstrate that the quasianalytical method can be used accurately to obtain such coefficients in the transonic flight regime.

Conclusion

Based upon these investigations and results, it is concluded that the quasianalytical method is a feasible approach for accurately obtaining transonic aerodynamic sensitivity coefficients in two dimensions. The results obtained from the quasianalytical method are almost identical to those obtained by the brute-force (finite-difference) technique. Furthermore, the study indicates that the computation of sensitivity derivatives at transonic conditions is generally more accurate using the quasianalytical direct solver approach than the finite-difference approach. In addition, the quasianalytical method is more efficient at supersonic Mach numbers and is potentially more efficient than the brute-force approach at transonic speeds. However, further studies to determine the effects of grid refinement and to examine the results over a wider range of design parameter variation are needed.

Acknowledgments

This effort was primarily supported by the National Aeronautics and Space Administration under Grant NAG 1-793 with E. Carson Yates, Jr. of the NASA Langley Research Center as Technical Monitor. A very warm and special thank you goes to M. S. Pilant, Professor of Mathematics, Texas A&M University, for helpful ideas and comments.

References

[1]Sobieski, J., "The Case for Aerodynamic Sensitivity Analysis," NASA/VPI&SY Symposium on Sensitivity Analysis in Engineering, Sept. 1986.

[2]Adelman, H. M., and Haftka, R. T., "Sensitivity Analysis and Discrete Structural Systems," *AIAA Journal,* Vol. 24, No. 5, May 1986, pp. 823–832.

[3]Bristow, D. R., and Hawk, J. D., "Subsonic Panel Method for Designing Wing Surfaces from Pressure Distributions," NASA CR-3713, 1983.

[4]Elbanna, H. M., "Numerical Computation of Aerodynamic Sensitivity Coefficients in the Transonic and Supersonic Regimes," M.S. Thesis, Texas A&M University, College Station, TX, May 1988.

[5]Abbott, I. H., and Von Doenhoff, A. E., *Theory of Wing Sections,* Dover, New York, 1959.

[6]Vanderplaats, G. N., Hicks, R. M., and Murman, E. M., "Application of Numerical Optimization Techniques To Airfoil Design," NASA SP-047, Pt. II, March 1975, pp. 745–768.

[7]Ballhaus, W. F., Jameson, A., and Albert, J., "Implicit Approximate Factorization Schemes for Steady Transonic Flow Problems," *AIAA Journal,* Vol. 16, No. 6, 1978, pp. 573–579.

[8]Gupta, S. K., and Tanji, K. K., "Computer Program for Large, Sparse, Unsymmetric Systems of Linear Equations," *International Journal for Numerical Methods in Engineering,* Vol. 11, 1977, pp. 1251–1259.

[9]Pissanetzky, S., *Sparse Matrix Technology,* Academic, New York, 1984.

[10]Press, W. H., Flannery, B. P., Tenkolsky, S. A., and Vetterling, W. T., *Numerical Recipes,* Cambridge Univ., Cambridge, MA, 1986.

[11]Elbanna, H. M., and Carlson, L. A., "Determination of Aerodynamic Sensitivity Coefficients in the Transonic and Supersonic Regimes," AIAA Paper 89-0532, Jan. 1989.